

Supporting Information for
Atmospheric Hydroxyl Radical Source: Reaction of Triplet SO₂ and Water

Authors:

Jay A. Kroll^{1,2,#}, Benjamin N. Frandsen^{3,#}, Henrik G. Kjaergaard^{3,*}, and Veronica Vaida^{1,2,*}

Affiliations:

¹Department of Chemistry and Biochemistry, University of Colorado Boulder, UCB 215,
Boulder CO 80309

²Cooperative Institute for Research in Environmental Sciences, University of Colorado Boulder,
UCB 216, Boulder CO 80309

³Department of Chemistry, University of Copenhagen, Universitetsparken 5, DK-2100,
Copenhagen Ø, Denmark

#Joint First Authors

*Corresponding Authors:

Veronica Vaida: vaida@colorado.edu

Henrik G. Kjaergaard: hgk@chem.ku.dk

S.1 Kinetics Analysis – Reaction of $^3\text{SO}_2$ with Methane

S.1.1 Photoexcitation Rate Constant, J, for Sulfur Dioxide

The Lamp spectrum shown in Figure S1 was measured using an International Light spectroradiometer at a resolution of 1 nm. The Absorption spectrum shown is from Manatt and Lane.¹ This spectrum was chosen for its close match to the resolution of the radiometer used to measure the flux of the lamp (0.1 nm). The flux and spectra shown here (Figure S1) were used to calculate the concentration of electronically excited SO_2 in the cell. The Xe Arc lamp used as a photochemical light source was filtered using a 280 nm longpass filter. This filter was chosen to allow maximum excitation of the electronic band found in the 250-340 nm region to increase the effect measured in our experiments while still preventing excitation of the photolytic band at shorter wavelengths.² It should be noted that the flux present in the Earth's troposphere does not extend below 300 nm but still has sufficient overlap with the transition to lead to electronic excitation of SO_2 in the atmosphere. Additionally, the wavelengths of light shorter than 300 nm used in this experiment are widely available above the ozone layer of Earth, the middle atmosphere of Venus, the troposphere of early Earth, and other planetary atmospheres where the chemistry described in the manuscript may play a role.

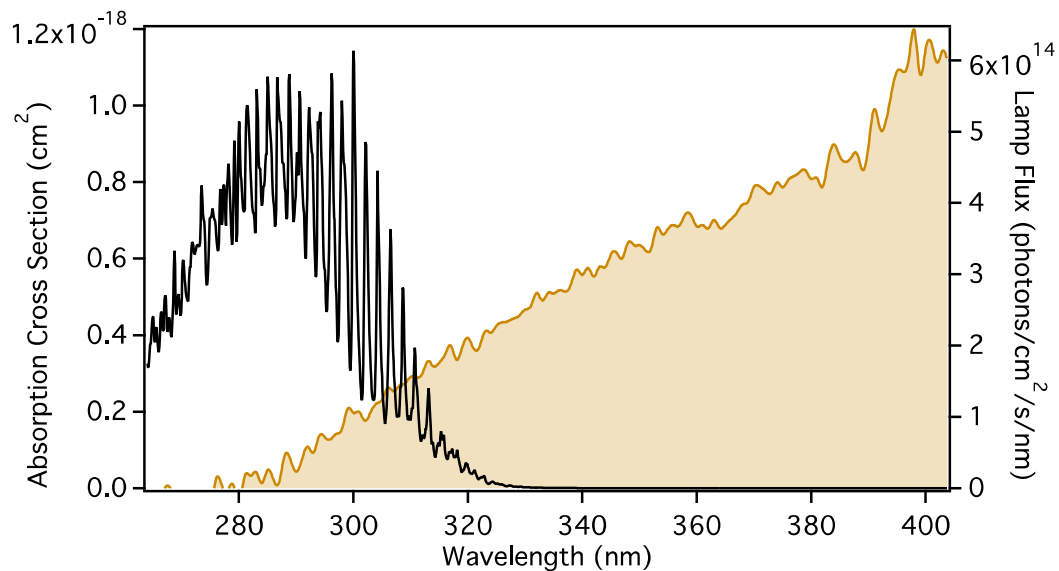


Figure S1. Flux from the 280 nm Filtered UV lamp (right axis) overlaid on absorption spectrum of SO_2 (left axis)

Typically rate constants for photo-excitation (J values) are calculated using the equation:

$$J = \int_{\lambda_1}^{\lambda_2} F(\lambda) * \sigma(\lambda) * \Phi(\lambda) d\lambda , \quad \text{eq. S1}$$

where $F(\lambda)$ is the photon flux, $\sigma(\lambda)$ is the absorption cross section, and $\Phi(\lambda)$ is the quantum yield ($\Phi = 1$ for direct excitation processes). This equation, however, assumes that the photon flux through the cell is constant. In our experiments, the concentration of SO_2 is large enough that the cell is opaque to wavelengths less than ~ 320 nm (Figure S2). Therefore, the flux is not constant throughout the cell but instead follows a decaying gradient through the cell as it is absorbed by SO_2 .

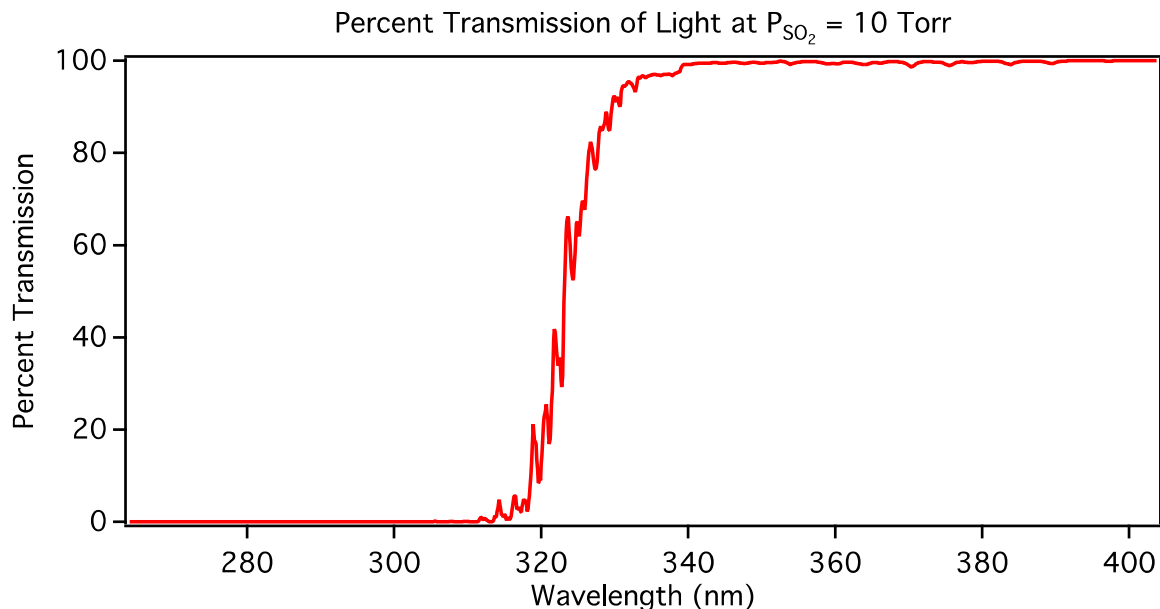


Figure S2. Percent transmission through a photochemical cell with a length of 50.165 cm containing SO_2 at a pressure of 10 Torr.

Due to the opacity of the cell, the rate constants for the photoexcitation of SO_2 to singlet and triplet SO_2 were obtained instead by calculating the average number of photons absorbed per cubic centimeter in the cell and dividing by the concentration of SO_2 . Because the concentration of SO_2 in the cell changes slightly over the course of the experiment, the values of J_1 (singlet) and J_3 (triplet) were calculated for each time step using equations S2 and S3,

$$J_1 = \frac{1}{l_{cell}*[SO_2]} \int_{\lambda=267 \text{ nm}}^{\lambda=340 \text{ nm}} F(\lambda) * (1 - e^{-\sigma(\lambda)*[SO_2]*l_{cell}}) d\lambda \quad \text{Eq. S2}$$

$$J_3 = \frac{1}{l_{cell}*[SO_2]} \int_{\lambda=340 \text{ nm}}^{\lambda=400 \text{ nm}} F(\lambda) * (1 - e^{-\sigma(\lambda)*[SO_2]*l_{cell}}) d\lambda , \quad \text{Eq. S3}$$

where $F(\lambda)$ is the flux of the lamp as a function of wavelength, $\sigma(\lambda)$ is the absorption cross section of SO_2 as a function of wavelength, $[SO_2]$ is the concentration of SO_2 in molecules/cm³, and l_{cell} is the length of the cell in centimeters. The J value for the direct excitation to the triplet state, J_3 , can be calculated using either equation S1 or S3 because the region of the spectrum from 340 to 400 nm is not saturated. Under these conditions, the two equations are equivalent

and yield the same value. The J values determined for our experimental set up are given in Table S1. Using the value for J_1 determined from equation S2 gives the average rate of production of $^1\text{SO}_2$ in the beam of UV light across the width of the cell. While the actual distribution of excited SO_2 in the cell will be a gradient due to the opacity of the SO_2 gas, the cell is well mixed on the timescale of the spectroscopic method and the depletion of methane measured represents reaction of methane with the average concentration of $^3\text{SO}_2$ in the UV beam.

Table S1. List of reactions in the kinetics scheme used to describe our system.

Reaction	Rate Constant	Value ^a	units
$\text{SO}_2 + \text{h}\nu \rightarrow ^1\text{SO}_2$	J_1	2.5×10^{-4}	s^{-1}
$\text{SO}_2 + \text{h}\nu \rightarrow ^3\text{SO}_2$	J_3	2.2×10^{-6}	s^{-1}
$^1\text{SO}_2 \rightarrow \text{SO}_2 + \text{h}\nu$	k_2	2.2×10^4	s^{-1}
$^1\text{SO}_2 \rightarrow ^3\text{SO}_2$	k_3	1.5×10^3	s^{-1}
$^1\text{SO}_2 + \text{SO}_2 \rightarrow \text{SO}_2 + \text{SO}_2$	k_4	2.9×10^{-11}	$\text{cm}^3 \text{ molec}^{-1} \text{ s}^{-1}$
$^1\text{SO}_2 + \text{SO}_2 \rightarrow ^3\text{SO}_2 + \text{SO}_2$	k_5	3.0×10^{-12}	$\text{cm}^3 \text{ molec}^{-1} \text{ s}^{-1}$
$^1\text{SO}_2 + \text{SO}_2 \rightarrow \text{SO} + \text{SO}_3$	k_6	4×10^{-12}	$\text{cm}^3 \text{ molec}^{-1} \text{ s}^{-1}$
$^3\text{SO}_2 \rightarrow \text{SO}_2 + \text{h}\nu$	k_7	1.1×10^3	s^{-1}
$^3\text{SO}_2 + \text{SO}_2 \rightarrow \text{SO}_2 + \text{SO}_2$	k_8	5.8×10^{-13}	$\text{cm}^3 \text{ molec}^{-1} \text{ s}^{-1}$
$^3\text{SO}_2 + \text{SO}_2 \rightarrow \text{SO} + \text{SO}_3$	k_9	7×10^{-14}	$\text{cm}^3 \text{ molec}^{-1} \text{ s}^{-1}$
$^1\text{SO}_2 + \text{M} \rightarrow \text{SO}_2 + \text{M}$	k_{10}	1×10^{-11} (approx.)	$\text{cm}^3 \text{ molec}^{-1} \text{ s}^{-1}$
$^1\text{SO}_2 + \text{M} \rightarrow ^3\text{SO}_2 + \text{M}$	k_{11}	1×10^{-12} (approx.)	$\text{cm}^3 \text{ molec}^{-1} \text{ s}^{-1}$
$^3\text{SO}_2 + \text{M} \rightarrow \text{SO}_2 + \text{M}$	k_{12}	1.1×10^{-13}	$\text{cm}^3 \text{ molec}^{-1} \text{ s}^{-1}$
$\text{SO} + \text{SO}_3 \rightarrow 2\text{SO}_2$	k_{13}	1.0×10^{-15}	$\text{cm}^3 \text{ molec}^{-1} \text{ s}^{-1}$
$^3\text{SO}_2 + \text{CH}_4 \rightarrow \text{Products}^b$	k_{14}	$\leq 2.9 \times 10^{-16}$	$\text{cm}^3 \text{ molec}^{-1} \text{ s}^{-1}$

^aAll rate constants are taken from Whitehill and Ono, 2012³ with the exception of J_1 and J_3 which were calculated using the experimental data obtained in this study and k_{13} which was taken from Chung, Calvert, and Bottenheim, 1975.⁴ Rate constants k_{10} and k_{11} are approximate and have not been experimentally measured. While taken from Whitehill and Ono, k_{12} also represents an approximation given the variety of species, which will each quench $^3\text{SO}_2$ differently. Note that M is any molecule other than SO_2 .

^bThis work and the given value is an upper limit.

S.1.2 Concentration of $^1\text{SO}_2$ and $^3\text{SO}_2$ in our experiment.

The electronically excited states of SO_2 (triplet and singlet) have short lifetimes, and the populations of these states can be assumed to be at a steady state, where the formation of newly excited $^1\text{SO}_2$ and $^3\text{SO}_2$ is matched by the loss of these molecules due to radiative and collisional relaxation or reaction. The relevant reactions are shown in Table S1 and the relationship can be described by the equations:

$$\begin{aligned} \frac{d[{}^1\text{SO}_2]}{dt} = 0 = & J_1[\text{SO}_2] - k_2[{}^1\text{SO}_2] - k_3[{}^1\text{SO}_2] - k_4[{}^1\text{SO}_2][\text{SO}_2] - k_5[{}^1\text{SO}_2][\text{SO}_2] \\ & - k_6[{}^1\text{SO}_2][\text{SO}_2] - k_{10}[{}^1\text{SO}_2][M] - k_{11}[{}^1\text{SO}_2][M] \end{aligned} \quad \text{Eq. S4}$$

$$\begin{aligned} \frac{d[{}^3\text{SO}_2]}{dt} = 0 = & J_3[\text{SO}_2] + k_3[{}^1\text{SO}_2] + k_5[{}^1\text{SO}_2][\text{SO}_2] + k_{11}[{}^1\text{SO}_2][M] - k_7[{}^3\text{SO}_2] \\ & - k_8[{}^3\text{SO}_2][\text{SO}_2] - k_9[{}^3\text{SO}_2][\text{SO}_2] - k_{12}[{}^3\text{SO}_2][M] - k_{14}[{}^3\text{SO}_2][\text{CH}_4] \end{aligned} \quad \text{Eq. S5}$$

Solving equations S4 and S5 for the concentrations of $^1\text{SO}_2$ and $^3\text{SO}_2$ respectively gives the following:

$$[{}^1\text{SO}_2] = \frac{J_1[\text{SO}_2]}{k_2 + k_3 + k_4[\text{SO}_2] + k_5[\text{SO}_2] + k_6[\text{SO}_2] + k_{10}[M] + k_{11}[M]} \quad \text{Eq. S6}$$

$$[{}^3\text{SO}_2] = \frac{J_3[\text{SO}_2] + k_3[{}^1\text{SO}_2] + k_5[{}^1\text{SO}_2][\text{SO}_2] + k_{11}[{}^1\text{SO}_2][M]}{k_7 + k_8[\text{SO}_2] + k_9[\text{SO}_2] + k_{12}[M] + k_{14}[\text{CH}_4]} \quad \text{Eq. S7}$$

S.1.3 Determination of k_{14} The rate constant for the reaction of $^3\text{SO}_2$ with methane (k_{14}) was determined by increasing the concentration of SO_2 in the cell, such that collisions with SO_2 dominated the relaxation processes for singlet and triplet SO_2 . This ensured that the concentration of $^3\text{SO}_2$ remained relatively constant during the course of the experiment and the reaction rate constant could be calculated using pseudo first order kinetics. The natural logarithm of the concentration of methane was plotted, and a line was fit to the data. The rate constant, k_{14} , could then be calculated using the equation,

$$m = -k_{14} [^3\text{SO}_2] \quad \text{Eq. S8}$$

where m is the slope of the fit line and $[^3\text{SO}_2]$ is the concentration of triplet state excited SO_2 in units of molecules/cm³. The concentration of $^3\text{SO}_2$ was determined using equation S7. Because the concentration depends on k_{14} , initially k_{14} was set to zero and $[^3\text{SO}_2]$ was calculated ignoring any depletion of $^3\text{SO}_2$ due to reaction with methane. The average concentration of $^3\text{SO}_2$ over the course of the experiment was then used to calculate k_{14} using equation S8. This rate constant was then substituted back into equation S7 and a new concentration of $^3\text{SO}_2$ was calculated. This process was repeated iteratively until the value of k_{14} converged. The rate constant was small enough that the value of k_{14} converged after just two iterations of this process to a value of $2.9 \times 10^{-16} (\pm 4.7 \times 10^{-16}) \text{ cm}^3 \text{ molecules}^{-1} \text{ s}^{-1}$. However, it should be noted that the fit slope, m , has a large standard deviation and cannot be statistically distinguished from zero (Figure S3, Table S2). Thus the error on the k_{14} is large and likewise, the rate constant is not statistically different from zero. Therefore, this rate constant should be treated as an upper limit.

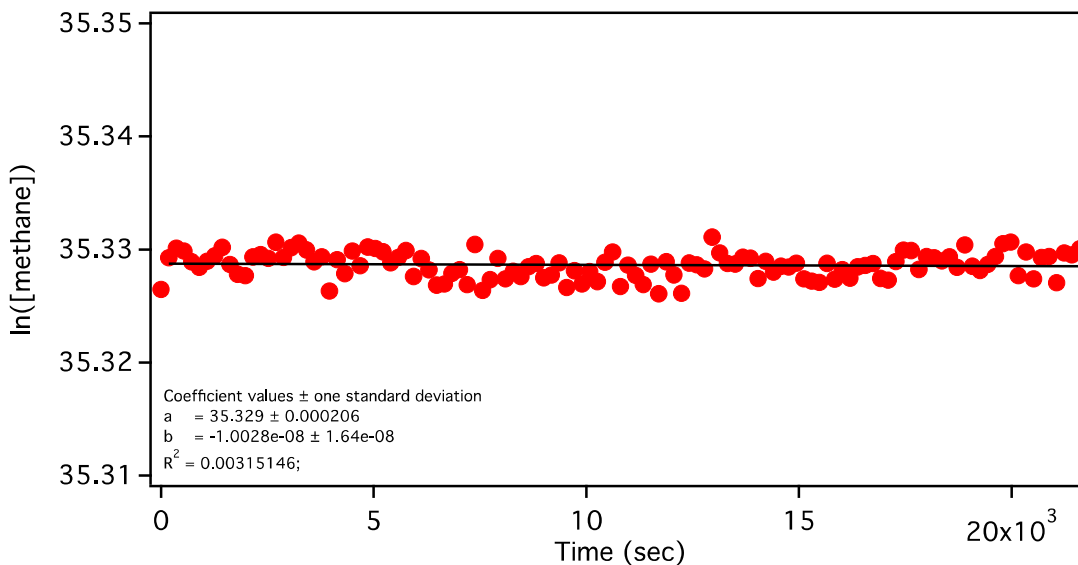


Figure S3. Linear fit of the $\ln([CH_4])$ vs time (where $[CH_4]$ is in molecules/cm³) used to determine the rate constant for reaction with ³SO₂ and methane, using pseudo first order kinetics and the ³SO₂ concentration.

Table S2. Rate constant (k_{14}) determined for the reaction of CH₄ with ³SO₂.

$m (\pm 1\sigma)^a$ (s ⁻¹)	[¹ SO ₂] ^b (molecules cm ⁻³)	[³ SO ₂] ^b (molecules cm ⁻³)	k_{14} (cm ³ molec ⁻¹ s ⁻¹)
-1.00×10^{-8} ($\pm 1.6 \times 10^{-8}$)	6.89×10^6	3.51×10^7	2.9×10^{-16} ($\pm 4.7 \times 10^{-16}$)

^aThe slope (m) including one standard deviation.

^bAverage concentration of ¹SO₂ (¹A₂) and ³SO₂ in the cell over the course of the photochemical excitation.

S.2 Kinetics Analysis – Reaction of $^3\text{SO}_2$ with Water

We did two experiments under wet conditions, a low and high methane concentration. The formation of OH in the reaction of $^3\text{SO}_2$ and H_2O is followed by observing the methane concentration, with the OH radicals assumed to be consumed by the methane scavenger molecules ($k_2 \sim 9.4 \times 10^{-15} \text{ cm}^3 \text{ molec}^{-1} \text{ s}^{-1}$ at $P_{\text{total}} = 10 \text{ Torr}$).



The $^3\text{SO}_2$ reaction with methane is competing, however we observed this reaction is observed to be slow.



In addition to these three reactions, the reaction of OH with SO_2 to form HOSO_2 (reaction S4) and the back reaction (reaction S5) may play a role at the pressures observed in the experiments ($P_{\text{total}} \sim 10 \text{ Torr}$). At 10 Torr, the rate constants for these two reactions are $k_4 \sim 2 \times 10^{-14} \text{ cm}^3 \text{ molecule}^{-1} \text{ s}^{-1}$ and $k_5 \sim 2 \times 10^{-6} \text{ s}^{-1}$ respectively.⁵



Under the conditions of the experiment, there are a number of potential side reactions that may interfere with determination of the rate constant for reaction S1. As noted in the main text, atmospheric O_2 leaking into the cell over time will have a significant effect on reaction S5 as it can react with HOSO_2 to form HO_2 and SO_3 ⁶ making the formation of HOSO_2 a permanent sink of OH. While there may be additional complicating reactions, this provides us with two limiting cases that provide insight into the bounds of the rate constant. The first case (case 1) assumes

that the dissociation of HOSO₂ is negligible and the reaction of OH with SO₂ to form HOSO₂ is strictly a sink of OH. In this case, hydroxyl radical is likely consumed as it is created and a steady state approximation for the concentration of OH can be made.

$$\frac{d[OH]}{dt} = 0 = k_1[H_2O][^3SO_2] - k_2[CH_4][OH] - k_4[OH][SO_2] \quad \text{Eq. S9}$$

This equation can be rearranged, solving for [OH] to give:

$$[OH] = \frac{k_1[^3SO_2][H_2O]}{k_2[CH_4] + k_4[SO_2]} \quad \text{Eq. S10}$$

In our experiments, we measured the rate of depletion of CH₄. This rate can be approximated by a linear fit of a plot of the concentration of methane vs. time. The slope of this line (b) is equal to the rate of change of the concentration of methane.

$$\frac{d[CH_4]}{dt} = b = -k_2[OH][CH_4] - k_3[^3SO_2][CH_4] \quad \text{Eq. S11}$$

Rearranging this equation gives:

$$-k_2[OH][CH_4] = b + k_3[^3SO_2][CH_4] \quad \text{Eq. S12}$$

Equations S10 and S12 can then be substituted into equation 9 to yield:

$$0 = k_1[^3SO_2][H_2O] + b + k_3[^3SO_2][CH_4] - k_4[SO_2] \frac{k_1[^3SO_2][H_2O]}{k_2[CH_4] + k_4[SO_2]} \quad \text{Eq. S13}$$

We can rearrange equation S13, solving for k₁ to give

$$k_1 = \frac{-b - k_3[^3SO_2][CH_4]}{[^3SO_2][H_2O] - \frac{k_4[SO_2][^3SO_2][H_2O]}{k_2[CH_4] + k_4[SO_2]}} \quad \text{Eq. S14}$$

In the second case (case 2), we can assume that there is little atmospheric O₂ contamination present and the pressure in the cell is low enough such that collisional stabilization of HOSO₂ is not efficient and the back reaction to form HO and SO₂ (reaction S5) is fast enough such that HOSO₂ is at steady state.

$$k_4[OH][SO_2] = k_5[HOSO_2] \quad \text{Eq. S15}$$

In this case, the concentration of OH can still be assumed to be at steady state, which is described by equation S16.

$$\frac{d[OH]}{dt} = 0 = k_1[H_2O][^3SO_2] - k_2[CH_4][OH] - k_4[OH][SO_2] + k_5[HOSO_2] \quad \text{Eq. S16}$$

Equation S15 informs us that the last two terms of this equation are equal and cancel each other out. Solving for k_1 then gives:

$$k_1 = \frac{k_2[CH_4][OH]}{[H_2O][^3SO_2]} \quad \text{eq. S17}$$

Rearranging equation S12 and substituting in for $k_2[CH_4][OH]$ gives:

$$k_1 = \frac{-b - k_3[CH_4][^3SO_2]}{[H_2O][^3SO_2]} \quad \text{Eq. S18}$$

In figures S4 and S5, we show the linear fit to the depletion of methane in the experiments under wet ($P[H_2O] \approx 3.5$ Torr) conditions with low and high methane concentration, respectively.

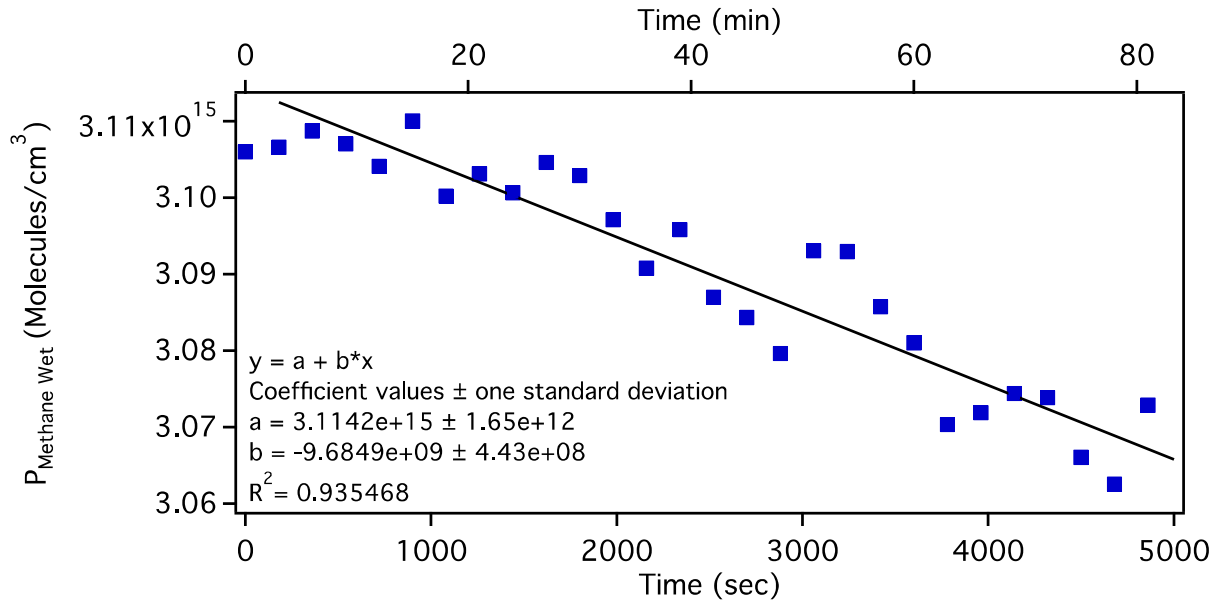


Figure S4. Linear fit to the depletion of methane in the low concentration CH_4 experiment under wet conditions.

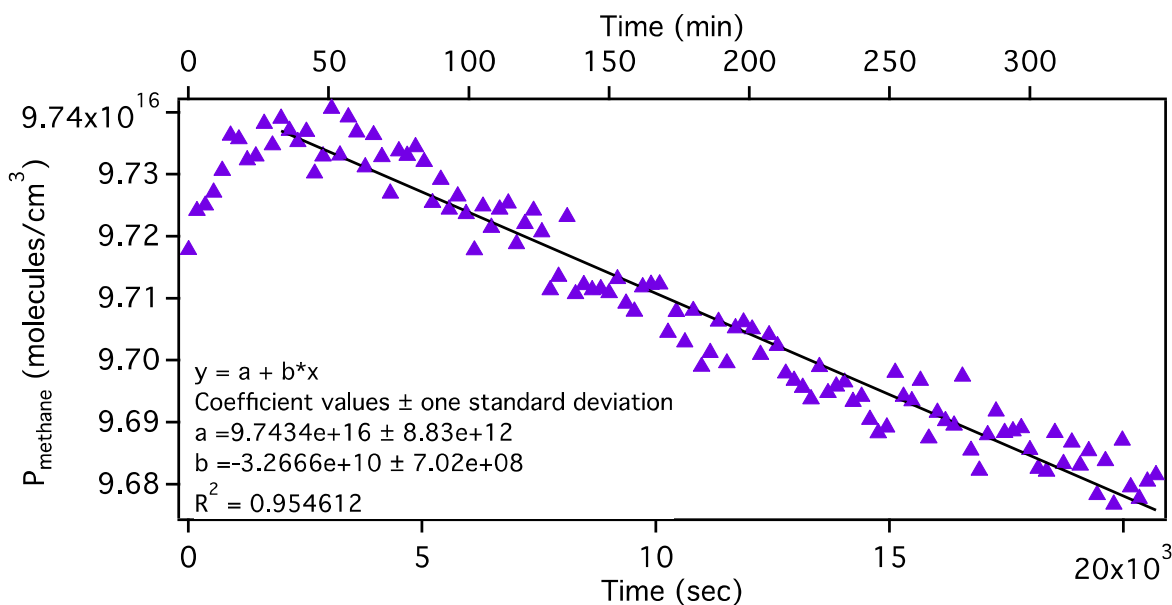


Figure S5. Linear fit of the depletion of methane in the high concentration CH₄ experiment under wet conditions.

Table S3. Concentrations of species in the wet photochemical experiments

Molecule	Low Methane Experiment (molecules/cm ³)	High Methane Experiment (molecules/cm ³)
SO ₂	1.42 x 10 ¹⁷	1.05 x 10 ¹⁷
H ₂ O	1.15 x 10 ¹⁷	1.145 x 10 ¹⁷
³ SO ₂	5.20 x 10 ⁷	5.34 x 10 ⁷
CH ₄	3.08 x 10 ¹⁵	9.97 x 10 ¹⁶

Using the fit slopes of the experimentally observed decay of methane along with the initial concentrations of each molecules in the experiment, equations S14 and S18 can be used to estimate upper bound (case 1) and lower bound (case 2) for the rate constant. Assuming the upper limit of the reaction of ³SO₂ with methane ($k_3 = 2.9 \times 10^{-16} \text{ cm}^3 \text{ molec}^{-1} \text{ s}^{-1}$) equation S18 (case 2) gives an lower limit on the rate constant $k_I = 1.6 \times 10^{-15} \text{ cm}^3 \text{ molecules}^{-1} \text{ s}^{-1}$ and $k_I = 5.1 \times 10^{-15} \text{ cm}^3 \text{ molecules}^{-1} \text{ s}^{-1}$, for the low methane and high methane experiments respectively. Using equation S14 (case 1) gives a upper limit on the rate constant $k_I = 1.6 \times 10^{-13} \text{ cm}^3 \text{ molec}^{-1} \text{ s}^{-1}$ and $k_I = 1.6 \times 10^{-14} \text{ cm}^3 \text{ molec}^{-1} \text{ s}^{-1}$, for the low methane and high methane experiments respectively.

This suggests that higher concentration methane experiment, which had less interference and a lower leak rate from atmospheric gasses better constrains the calculation of the rate constant for reaction S1. This suggests that the true rate constant, k_1 , has a value between $5-16 \times 10^{-15}$ $\text{cm}^3\text{molec}^{-1}\text{s}^{-1}$.

The difference in rate constants in the low and high methane experiments, suggests that the steady state concentration of OH may be a poor assumption, there are wall losses that are unaccounted for, and/or secondary chemistry is occurring in the cell, which we are not monitoring for. In particular we are not accounting for a second channel of HOSO₂ decay which generates O atoms⁷ that can react with H₂O to generate additional OH radicals. Also, we are not accounting for any secondary chemistry with the HOSO radical or the CH₃ radicals that are formed in the cell. The current experiments do not provide pressure or temperature dependence for the rate constant and do not account for secondary chemistry such as reaction involving HOSO. This would suggest that the errors on these measured rate constants are large and should be treated with caution. They may nevertheless be compared with the calculated rates.

S.3 – Computational Details and Results

The reactions S1-S3 were studied theoretically at the ω B97X-D level of theory with the aug-cc-pVTZ for all non-sulfur atoms and aug-cc-pV(T+d)Z for sulfur atoms (ω B97X-D/ aug-cc-pV(T+d)Z).⁸ All calculations used Gaussian16 Rev A.03.⁹ Subsequently single point energies of the stationary points were calculated with the coupled cluster including singles, doubles and perturbative triples CCSD(T) method and the same basis set. Unrestricted calculations were performed on all species. ω B97X-D optimizations of structures were followed by harmonic frequency calculations that were used to calculate zero-point vibrational energy (ZPVE) corrections. Exactly one imaginary frequency was found for the transition states (TS) and, no imaginary frequencies for the minima.

Intrinsic reaction coordinate (IRC) calculations were carried out to connect the transition state to both reactants and products. The reactions are going from reactants to a reaction complex (RC) *via* the TS to a product complex (PC) and finally the products. The IRCs connect the TS with the RC and PC complexes. The reactive complex is formed from collision of the reactants and the products arise as the product complex dissociate. To ensure IRC calculations ran all the way to the minimum the keyword maxpoints=1000 was used. Furthermore, for some transition state optimizations and IRC calculations, the scf=qc keyword was used because calculations would otherwise not converge.

We have used Transition State Theory (TST) from RC *via* TS to PC to calculate the reaction rate. Also since a H atom is transferred quantum tunneling correction is important and was included using one dimensional Eckart tunneling.¹⁰ Partition functions necessary in TST were computed using the calculated harmonic frequencies with the approximations to statistical mechanics inherent in the Gaussian16 program.⁹

$$k_{TST} = \frac{k_B T}{h} \frac{Q_{TS}}{Q_{RC}} \exp\left(\frac{-\Delta E_{TS-RC}}{RT}\right), \quad \text{eq.(S13)}$$

where Q is the partition function, ΔE the energy difference including ZPVE between TS and RC. The equilibrium constant K_{eq} between the reactants and the RC is included in the calculated bimolecular rate constant.

$$k_{bimolec} = k_{TST} \frac{K_{eq}}{c^o} = \frac{k_{TST}}{c^o} \exp\left(\frac{-\Delta G_{RC-R}}{RT}\right), \quad \text{eq.(S14)}$$

The equilibrium constant is found from the Gibbs free energies, and the standard concentration, c^o , is 2.4×10^{19} molecules cm^{-3} .

The calculated barriers, energy of reaction, tunneling correction and rates for the three reactions investigated are given in Tables S3-S5, for the different theoretical methods. The accuracy of the calculations was assessed by calculation of the reaction methane with OH, for which experimental rate constants are available. The methane + OH reaction (rxn.S2) is our probe for OH production. This reaction has been studied extensively in the literature both experimentally and theoretically.²⁻⁶ At 295K the recommended experimental rate constant of this reaction is $k = 5.97 \times 10^{-15}$ $\text{cm}^3 \text{molecules}^{-1} \text{s}^{-1}$.¹¹ Our CCSD(T)/aug-cc-pV(T+d)Z// ω B97X-D/aug-cc-pV(T+d)Z calculated rate constant at 298K is $k = 9 \times 10^{-14}$ $\text{cm}^3 \text{molecules}^{-1} \text{s}^{-1}$, which suggests that our calculated rate constants provide estimates of the reaction rate constants that are likely within two orders of magnitude of the experimental rate constants. The TST calculated rates on low barrier bimolecular reactions are not expected to be accurate but do provide qualitative support of the experiments.

Table S4. Calculated rates and parameters at the ω B97X-D/aug-cc-pV(T+d)Z level.

Reaction	E_{R-TS}^a	E_{RC-TS}^a	E_{TS-PC}^a	ν_{imag}^b	κ^c	k^d	$\Delta E_{rxn} (R \text{ to } P)^a$
$^3SO_2 + H_2O$	2.4	5.2	6.3	1497i	8.8	1.1×10^{-14}	2.7
$OH + CH_4$	2.2	-	14.9	1102i	4.0	5.2×10^{-12}	-12.7
$^3SO_2 + CH_4$	1.3	1.7	13.9	335i	1.1	4.2×10^{-13}	-10.0

^aEnergies include ZPVE and are given in kcal mol⁻¹.

^b Imaginary frequency of the TS in cm⁻¹

^c Eckart quantum tunneling (unitless) of RC to TS to PC barrier.

^d Rate constant at 298.15K for the forward reaction from R to TS in cm³molecules⁻¹s⁻¹ including tunneling.

Table S5. Calculated rates and parameters at the CCSD(T)/aug-cc-pV(T+d)Z// ω B97X-D/aug-cc-pV(T+d)Z level.

Reaction	E_{R-TS}^a	E_{RC-TS}^a	E_{TS-PC}^a	ν_{imag}^b	κ^c	k^d	$\Delta E_{rxn} (R \text{ to } P)^a$
$^3SO_2 + H_2O$	4.8	4.8	4.9	1497i	8.0	1.7×10^{-16}	2.7
$OH + CH_4$	5.0	-	18.5	1102i	8.4	9.0×10^{-14}	-13.4
$^3SO_2 + CH_4$	3.8	4.9	16.8	335i	1.1	6.2×10^{-15}	-10.7

^a Energies include ZPVE and are given in kcal mol⁻¹.

^b Imaginary frequency of the TS in cm⁻¹

^c Eckart quantum tunneling (unitless) of RC to TS to PC barrier.

^d Rate constant at 298.15K for the forward reaction from R to TS, in cm³molecules⁻¹s⁻¹, including tunneling.

The identification of the mechanism for the $^3\text{SO}_2 + \text{H}_2\text{O}$ reaction qualitatively shows that photoexcitation of SO_2 can cause OH formation. The $\omega\text{B97X-D/aug-cc-pV(T+d)Z}$ IRC connecting the TS to either the reactant complex (RC, left) or the product complex (PC, right) is shown in Figure S6. The ZPVE corrected $\text{CCSD(T/aug-cc-pV(T+d)Z//}\omega\text{B97X-D/aug-cc-pV(T+d)Z}$ energy difference between the R and TS is 4.8 kcal/mol, which leads to a calculated rate constant of $2 \times 10^{-16} \text{ cm}^3 \text{ molecule}^{-1} \text{ s}^{-1}$.

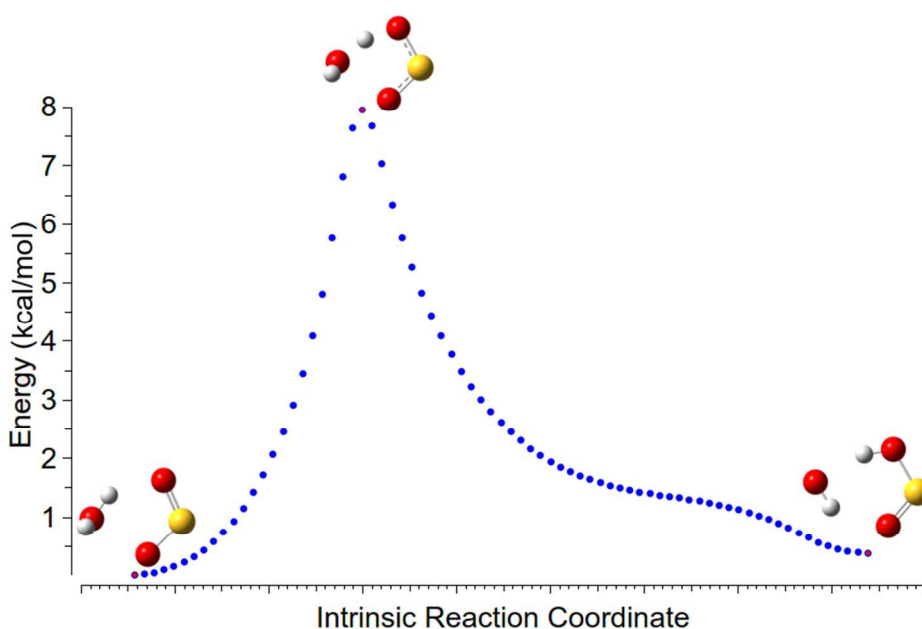


Figure S6. The $\omega\text{B97X-D/aug-cc-pV(T+d)Z}$ (no ZPVE) calculated Intrinsic Reaction Coordinate (IRC) of the $^3\text{SO}_2 + \text{H}_2\text{O}$ reaction. To the left is shown the reactive complex (RC) and to the right the product complex (PC). Both of these complexes are held together by hydrogen bonds and van der Waals interactions.

The $^3\text{SO}_2$ can also react with methane although it was found experimentally to be very slow. The calculated IRC of the hydrogen abstraction reaction is shown in Figure S7. The ZPVE corrected $\text{CCSD(T/aug-cc-pV(T+d)Z//}\omega\text{B97X-D/aug-cc-pV(T+d)Z}$ energy difference between R and TS is 3.8 kcal/mol, which leads to a rate constant of $6 \times 10^{-15} \text{ cm}^3 \text{ molecule}^{-1} \text{ s}^{-1}$. This energy

barrier is similar to that of the $^3\text{SO}_2$ and H_2O reaction and some competition between these two reactions could exist. At our current level of calculations it is difficult to get an accurate estimate of this competition. The $^3\text{SO}_2 + \text{CH}_4$ is calculated to be relatively fast compared with $^3\text{SO}_2 + \text{H}_2\text{O}$ despite similar R to TS barriers, which mainly arise due to differences in the partition function. As shown in the main manuscript Figure 1, the reaction of $^3\text{SO}_2$ and methane is found experimentally to be very slow in the absence of water.

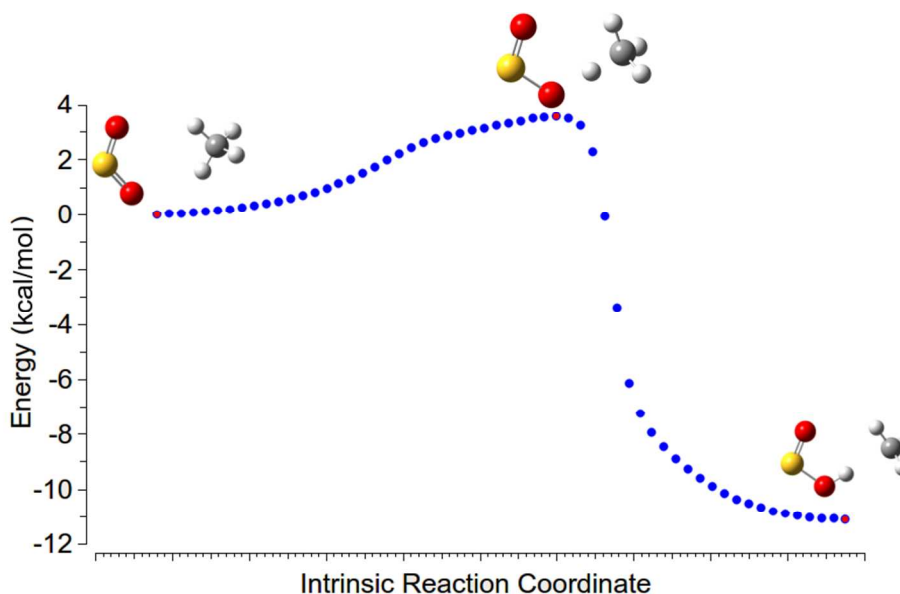


Figure S7. The $\omega\text{B97X-D/aug-cc-pV(T+d)Z}$ (no ZPVE) calculated Intrinsic Reaction Coordinate (IRC) of the $^3\text{SO}_2 + \text{CH}_4$ reaction. To the left is shown the pre-reactive complex (RC) and to the right the product complex (PC). Both of these complexes are held together by hydrogen bonds and van der Waals interactions.

S.6 – Computed structures and energies

Z-matrices of ω B97X-D/aug-cc-pV(T+d)Z optimized structures, in Cartesian coordinates

(Ångstrom):

$^3\text{SO}_2$:

S	0.0	0.0	0.3465114801
O	0.0	-1.3280489075	-0.3438812401
O	0.0	1.3280489075	-0.3438812401

OH :

O	1.3198362665	0.2587100046	-0.0003054206
H	1.1739087335	1.2176429954	0.0017604206

CH_4 :

C	0.0	0.0	0.0
H	0.628002	0.628002	0.628002
H	-0.628002	-0.628002	0.628002
H	-0.628002	0.628002	-0.628002
H	0.628002	-0.628002	-0.628002

H_2O :

O	0.2804283916	-1.3003320083	0.0
H	1.2369109713	-1.2636774726	0.0
H	-0.0042999723	-0.3864763091	0.0

HOSO :

S	-0.0311623931	0.5157662847	-0.1137222115
O	1.2502761631	-0.1869879017	-0.3055999596
O	-1.1953212883	-0.6046383638	0.1555862171
H	-0.7869764817	-1.4795680191	0.1317699539

CH_3 :

C	0.0	-0.0000001111	0.0
H	0.0	1.077975	0.0
H	-0.9335538309	-0.5389876667	0.0
H	0.9335538309	-0.5389876667	0.0

RC rxn 1 :

S	0.9995504719	-0.0734593	0.0057845702
O	0.3920357739	1.2876460638	0.0417832256
O	-0.1395116863	-1.1850229739	-0.0012067377
O	-2.0111715346	0.0121454766	-0.1010264365
H	-2.2031774963	-0.2581994662	0.8009378859
H	-1.4356735286	0.7942181997	-0.0269485075

TS rxn 1 :

S	1.0059709087	-0.0825678641	0.0013999421
O	0.220305447	1.2500748135	0.0276385644
O	-0.0500164466	-1.1919764612	-0.0091940079
O	-1.8328494762	0.054261458	-0.1078235887
H	-2.0184541581	-0.3455478663	0.7514821216
H	-0.9070632748	0.83781692	-0.0015990315

PC rxn 1 :

S	1.0700148864	-0.1200636769	-0.005561944
O	0.2574938867	1.2770056297	0.0153130823
O	0.1043828147	-1.2458874708	0.0458898563
O	-2.3285941934	0.1930904306	-0.0763709873
H	-1.80996016	-0.6384691428	-0.0329814212
H	-0.7089182344	1.1045302301	-0.0351065862

RC rxn 3 :

S	-1.4165741386	-0.1621890392	-0.2065409294
O	-0.6021634942	-1.4069440252	-0.0403146232
O	-0.8603544678	1.2250712005	-0.2891049048
C	2.5888794225	0.2747203931	-0.0020343123
H	3.1353471945	0.3427672118	-0.9402423104
H	3.2876280251	0.321451691	0.8305262429
H	2.0474402054	-0.6685630512	0.0335913264
H	1.8867538331	1.1030784292	0.0677002808

TS rxn 3 :

S	-1.1276252251	-0.1961482577	-0.0000038951
O	0.1542859137	-1.160851324	0.0000066065
O	-0.7616733795	1.2355633522	-0.0000097233
C	2.3621877689	0.2751309506	-0.0000014483
H	2.8927921026	-0.0049726843	-0.9051353345
H	2.8927999477	-0.004971752	0.9051281263
H	1.3947459145	-0.3715380252	0.0000032159
H	2.0413999573	1.3107367403	-0.0000005475

PC rxn 3 :

S	-1.1142672272	-0.1794207651	0.0000156102
O	0.1588589028	-1.1947718786	0.000018367
O	-0.6222977864	1.2120524071	-0.0000214795
C	2.7621333556	0.3910800269	0.0000013833
H	3.1356442857	-0.0054874878	-0.9322702586
H	3.1356367203	-0.0054990522	0.9322711526
H	0.9929392981	-0.6802056268	-0.0000114103
H	2.178629451	1.2996663764	0.0000046353

Table S6. ω B97X-D/aug-cc-pV(T+d)Z calculated energies and spin multiplicities

Molecule	E (hartree)	ZPVE (hartree)	Spin multiplicity	Thermal correction (hartree)
$^3\text{SO}_2$	-548.5343615	0.005335	2.01673	-0.020026
OH	-75.740745	0.008609	0.75292	-0.008308
CH ₄	-40.5200736	0.044846	0	0.027536
H ₂ O	-76.4399279	0.021657	0	0.004029
HOSO	-549.2275861	0.016767	0.75546	-0.010522
CH ₃	-39.8391759	0.029813	0.75396	0.011727
RC rxn 1	-624.9826333	0.030854	2.01340	0.001074
TS rxn 1	-624.9699706	0.026498	2.01265	-0.002260
PC rxn 1	-624.9820283	0.028520	2.00823	-0.003554
RC rxn 3	-589.0556605	0.050702	2.01674	0.011175
TS rxn 3	-589.0499562	0.047778	2.01459	0.015731
PC rxn 3	-589.0733109	0.049030	2.00959	0.014718

Table S7. CCSD(T)/aug-cc-pV(T+d)Z single point energies and spin multiplicities

Molecule	E (hartree)	Spin multiplicity
³ SO ₂	-547.8793943	2.09146
OH	-75.6455762	0.757087
CH ₄	-40.4409182	0
H ₂ O	-76.3422759	0
HOSO	-548.5701721	0.782578
CH ₃	-39.7636563	0.761743
RC rxn 1	-624.2254511	2.048819
TS rxn 1	-624.2135100	2.043747
PC rxn 1	-624.2233364	2.038302
RC rxn 3	-588.3225265	2.091849
TS rxn 3	-588.3118517	2.063271
PC rxn 3	-588.3399113	2.044098

Bibliography

1. Manatt, S. L.; Lane, A. L., A Compilation of the Absorption Cross-Sections of SO₂ from 106 to 403 nm, *Journal of Quantitative Spectroscopy and Radiative Transfer* **1993**, *50* (3), 267-276.
2. Okabe, H., Fluorescence and Predissociation of Sulfur Dioxide, *J. Am. Chem. Soc.* **1971**, *93* (25), 7095-7096.
3. Whitehill, A. R.; Ono, S., Excitation Band Dependence of Sulfur Isotope Mass-Independent Fractionation During Photochemistry of Sulfur Dioxide Using Broadband Light Sources, *Geochimica et Cosmochimica Acta* **2012**, *94* (Supplement C), 238-253.
4. Chung, K.; Calvert, J. G.; Bottenheim, J. W., The Photochemistry of Sulfur Dioxide Excited within Its First Allowed Band (3130 Å) and the “Forbidden” Band (3700–4000 Å), *Int. J. Chem. Kinet.* **1975**, *7* (2), 161-182.
5. Somnitz, H., Quantum Chemical and Dynamical Characterisation of the Reaction OH + SO₂ ⇌ HOSO₂ over an Extended Range of Temperature and Pressure, *Phys. Chem. Chem. Phys.* **2004**, *6* (14), 3844-3851.
6. Gleason, J. F.; Sinha, A.; Howard, C. J., Kinetics of the Gas-Phase Reaction HOSO₂ + O₂ → HO₂ + SO₃, *J. Phys. Chem.* **1987**, *91* (3), 719-724.
7. Egsgaard, H.; Carlsen, L.; Florencio, H., et al., Experimental Evidence for the Gaseous HSO₃• Radical. The Key Intermediate in the Oxidation of SO₂ in the Atmosphere, *Chemical Physics Letters* **1988**, *148* (6), 537-540.
8. Dunning, T. H. J.; Peterson, K. A.; Wilson, A. K., Gaussian Basis Sets for Use in Correlated Molecular Calculations. X. The Atoms Aluminum through Argon Revisited, *J. Chem. Phys.* **2001**, *114* (21), 9244-9253.
9. Frisch, M. J.; Trucks, G. W.; Schlegel, H. B., et al. *Gaussian 16, Revision A.03*, Gaussian, Inc.: Wallingford CT, 2016., 2016.
10. Eckart, C., The Penetration of a Potential Barrier by Electrons, *Phys. Rev.* **1930**, *35* (11), 1303-1309.
11. Vaghjiani, G. L.; Ravishankara, A. R., New Measurement of the Rate Coefficient for the Reaction of OH with Methane, *Nature* **1991**, *350* (6317), 406-409.